Transportation Research Part D 114 (2023) 103574

Contents lists available at ScienceDirect

Transportation Research Part D

journal homepage: www.elsevier.com/locate/trd

Pollution and noise reduction through missed approach maneuvers based on aircraft reinjection

Rafael Casado [a,*], Aurelio Bermúdez [a], Enrique Hernández-Orallo [b], Pablo Boronat [c], Miguel Pérez-Francisco [d], Carlos T. Calafate [b]

[a] Albacete Research Institute of Informatics, University of Castilla-La Mancha, C. de la Investigación 2, Albacete, 02071, Spain
[b] Department of Computer Engineering (DISCA), Universitat Politècnica de València, Camino de Vera, S/N, Valencia, 46022, Spain
[c] Computer Languages and Systems Department, Universitat Jaume I (UJI), Av. Sos Baynat S/N, Castelló de la Plana, 12071, Spain
[d] Computer Science and Engineering Department, Universitat Jaume I (UJI), Av. Sos Baynat S/N, Castelló de la Plana, 12071, Spain

ARTICLE INFO

Keywords:
Precision approach
Missed approach
Aircraft noise simulation
Civil aircraft pollution

ABSTRACT

Skyrocketing prices of fuel and increasing concerns towards achieving lower carbon footprints favor any improvements towards a greener transportation ecosystem. In this work we focus on missed approaches, which are forced maneuvers at the end of regular flights that generate significant noise and pollution levels near airports. In a previous work we introduced a reinjection technique for this maneuver able to substantially mitigate such negative effects. To confirm this point, in this work we compare this technique with a conventional procedure by using well-known models, such as the ECAC Doc. 29 noise model and the BADA aircraft performance model. A noise map at the ground level and a measure of the diffused pollutants have been obtained, confirming the lower ecological impact of the reinjection technique. Compared to the conventional maneuver, the reinjection-based approach obtains a reduction of about 80% in pollutant emissions, while the affected area for equivalent noise level thresholds is reduced to nearly half.

1. Introduction

Aircraft noise is a major problem in airport surroundings as it is directly perceived by neighboring citizens, causing regulations to gradually become more restrictive due to this kind of nuisance (ICAO, 2017). Fig. 1 illustrates the evolution of noise-related standards throughout the years, clearly highlighting these increased restrictions. However, aircraft noise is quite difficult to model due to the amount of concerning factors, such as multiple noise sources, distance and angles in the reception location, wind and other meteorological phenomena, or even ground obstacles. In addition, there are also different ways to define noise impact on a ground receptor, as it can be the maximum noise level, the accumulated received noise, or the noise equivalent level perceived over time.

At the same time, aircraft emissions are known to cause major ecological problems, both for their relation to climate change, and for the respiratory diseases they cause. In particular, aircraft emit different pollutants such as carbon monoxide (CO), carbon dioxide (CO_2), nitrogen oxides (NO_x), or sulfur oxides (SO_x), but also unburnt fuel and other particulates. For these undesired emissions there are straightforward equations relating them to fuel consumption, and obviously with the power demanded to the engines

* Corresponding author.
E-mail addresses: rafael.casado@uclm.es (R. Casado), Aurelio.Bermudez@uclm.es (A. Bermúdez), ehernandez@disca.upv.es (E. Hernández-Orallo), boronat@uji.es (P. Boronat), mperez@uji.es (M. Pérez-Francisco), calafate@disca.upv.es (C.T. Calafate).

https://doi.org/10.1016/j.trd.2022.103574
Received 25 July 2022; Received in revised form 3 November 2022; Accepted 12 December 2022
Available online 23 December 2022

Nomenclature

D	aerodynamic drag force (N)
C_D	drag coefficient
C_{D_0}	parasitic drag coefficient
C_{D_2}	induced drag coefficient
C_{f1}	1st trust specific fuel consumption coefficient (kg/(min ×kN))
C_{f2}	2nd trust specific fuel consumption coefficient (kt)
C_{f3}	3rd trust specific fuel consumption coefficient (kg/min)
C_{f4}	4th trust specific fuel consumption coefficient (ft)
F_t	fuel flow (kg/min) (as provided by the fuel consumption model)
g	gravitational acceleration (m/s^2)
h	geodetic altitude (m)
m	aircraft mass (kg)
T	engine thrust force (N)
V	true airspeed (m/s)
W	aircraft weight (N)
η	trust specific fuel flow (kg/(min ×kN))
T_s	aircraft spacing (s)
T_1	threshold time (for gap search) (s)
CO_2	carbon dioxide
SO_x	sulfur oxides
NO_x	nitrogen oxides
HC	hydrocarbons
CO	carbon monoxide
H_2O	water
E	amount of pollutant emissions (kg)
FF	fuel flow (kg/s) (as provided by the ICAO databank)
REI	reference emission index (g/kg fuel)
EI, EI_i	emission index (g/kg fuel)
W_f, W_{fi}	modeled or measured fuel flow (kg/s)
W_{ff}	corrected fuel flow (kg/s)
δ_{amb}	ratio of ambient pressure over sea level pressure
θ_{amb}	ratio of ambient temperature over sea level temperature
Ma	Mach number
H	humidity correction factor
SH	specific humidity
n_e	number of aircraft engines
t_i	period of time (s)
L_{max}	Maximum sound level (dB)
SEL (L_{AE})	Sound Exposure Level (dB)
NPD-data	Noise-power-Distance (NPD) data.

in each flight phase (DuBois and Paynter, 2006). The Base of Aircraft Data version 3 (BADA3) provides accepted models for fuel consumption (Poles et al., 2010; Harada et al., 2013).

Considering the aforementioned issues, we find that, nowadays, aviation industry (airlines, OEMS, regulators, etc.) usually face pressure to reduce the negative impact of flights, given that crowded airports are often close to important metropolitan areas. Specifically, when attempting to mitigate the negative impact of aircraft, we find that take-offs and landings are the two maneuvers which have a more important ecological impact and which, apart from technological improvements such as better engines or optimized fuselage, offer more room for pollution and noise reduction (Homola et al., 2019; Girvin, 2009).

In a previous work, we addressed these issues by proposing a reinjection method, which we called Aircraft Reinjection System (ARS) (Casado et al., 2021), applicable to missed approach maneuvers. The idea of this method consists of reserving or generating gaps in the flow of aircraft coming in to land and inserting the aircraft in one of these gaps in case of a missed approach. In contrast, in the classical procedure the affected aircraft is conducted outside the airport operation airspace, adopting a waiting state until the controllers find a gap in the flow; at that time, the aircraft completely re-initiates the landing procedure. Hence, our approach

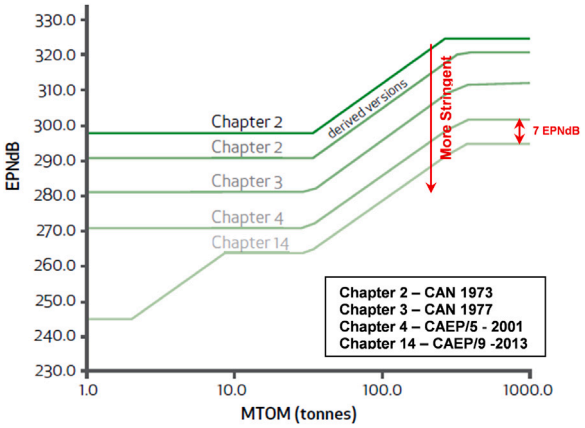

Fig. 1. Progression of the ICAO Noise Standards for aeroplanes when relating the maximum takeoff mass (MTOM) to the effective perceived noise (EPN). *Source:* Taken from (ICAO, 2022).

(ARS) allows the aircraft to land as soon as possible, thus avoiding the additional congestion on the airport airspace caused by the traditional maneuver. Obviously, both methods have to comply with International Civil Aviation Organization (ICAO) separation standards (ICAO, 2016).

The purpose of the present work is to compare the two missed approach methods in terms of their ecological impact on the surrounding area of an airport. The comparison is based on simulations of the specific case of the runway RWY 13 at the Málaga airport (Spain), but the results provide a quite general view. The noise model is an implementation of the European Civil Aviation Conference (ECAC) Doc. 29 (ECAC.CEAC, 2016a), and aircraft emissions are computed according to the Boeing Fuel Flow Method 2 (BFFM2) (DuBois and Paynter, 2006). Simulation results show that the proposed traffic reinjection system is able to reduce pollutant emissions such as CO_2, CO, HC, NO_x, or SO_x, by nearly 80% with respect to the conventional maneuver. Concerning noise, we find that the affected area can be quite significantly reduced, with a reduction of nearly 50% for the same noise thresholds.

The remainder of this paper is structured as follows. In the next section, we present some related works on this topic. In Section 3 we describe the conventional missed approach procedure and present an overview of our previously proposed solution (ARS), including a performance model and a fuel consumption model. Next, Section 4 details how the different pollutant emissions are computed. Details about the noise model adopted for the present study are then presented in Section 5. Afterwards, Section 6 presents the simulation methodology, as well as the results obtained in this work. Finally, the main conclusions and future works are drawn in Section 7.

2. Related work

Aircraft noise is one of the most harmful environmental effects on day-to-day life in airports' surroundings. It can cause a lot of well-known and unwanted problems: sleep problems, reduced children's academic performance, psychiatric diseases, metabolic diseases, cardiovascular diseases, etc. W.H.O. et al. (2011), Basner et al. (2017), Clark and Paunovic (2018). Noise can even limit the air traffic in and around many airports because of the increasing number of people exposed to it. Therefore, noise abatement techniques can help to improve the quality of life of many people and its coexistence with aerial facilities.

In addition, it is known that exposure to air pollution increases the risk of developing a wide range of health disorders. Many studies demonstrate that airports are a major source of environmental pollution. In particular, aircraft engine emissions contain large quantities of nano-sized particles that can easily reach the lower airways of living beings when inhaled (Bendtsen et al., 2021). Furthermore, they show that exposure to airport emissions is associated with biomarkers of exposure and biomarkers of effect on airport staff. An in-depth review of the air quality around airports activity is presented in Riley et al. (2021). In this review, it is shown that, in many studies, the concentrations of ultrafine particulate matter (UFP), as well as particulate matter under 2.5 μm of diameter, polycyclic aromatic hydrocarbons, and black carbon (among others) are elevated around airports, with the known effects on health of all these pollutants.

Focusing on the scope of the paper, many works have modeled or measured noise and pollutant emissions in landing maneuvers of civil aircraft. For instance, (Andarani et al., 2018; Filippone, 2017; Isermann and Bertsch, 2019; Simons et al., 2022) are devoted to noise, (Dancila et al., 2013; Chati and Balakrishnan, 2014; Murrieta-Mendoza and Botez, 2016; Zhou et al., 2019) are devoted to fuel consumption and gas emissions, and Mahashabde et al. (2011), Salah (2014), Rodríguez-Díaz et al. (2019) consider both emissions, pollutants and noise.

An interesting review of different models and techniques to study the aviation noise impact can be found in Isermann and Bertsch (2019). Noise models are classified as *best practice models* and *scientific models*. In best practice models, an aircraft is considered as a unified noise source, and they are based on aircraft performance and noise characteristics databases. This is the kind of model we

have used in the present work. In contrast, scientific models are more complex as the different elements of an aircraft are considered as separated noise sources.

In Andarani et al. (2018), a best practice model simulator is developed, and it is validated by comparing the results with real measures taken at six locations on the ground. Similar results are shown in Simons et al. (2022). In this paper, the authors compare simulation predictions obtained with the best practice model used in the Netherlands with real measurements taken at 40 points around the Schiphol Airport. With progressive noise abatement measures, their results show that, in 2012, simulations tended to underestimate noise effects; as time passed, they progressively become more coincident with real data, arriving in 2018 to a slight overestimation.

A recent paper (Meister et al., 2021) evaluates three different aircraft noise programs: sonAIR, FLULA2 and Aviation Environmental Design Tool (AEDT), comparing their results with real measurements. The conclusion is that they all match each other well and with the measurements. It should be noted that AEDT is compliant with the ECAC Doc. 29 noise model (ECAC.CEAC, 2016a), in which we have based our noise library.

Filippone has made important contributions to aircraft noise simulations. With respect to our work, his paper (Filippone, 2017) is of particular interest. The results show the benefits of noise reduction when modifying the steep approach or displacing the touch-down point in the landing maneuver. The work is based on a detailed scientific model presented in Filippone (2016). The introduced optimizations could be compatible with ARS.

Back in 2013 (Dancila et al., 2013) evaluated the cost in terms of fuel and pollution of missed approach procedures. In their work, the overrun due to the missed approach is evaluated by considering several possibilities such as having an aircraft being directed to a holding pattern, or having them redirected to one of the entry points in the approach procedure instead. When comparing the considered missed approach variants with a standard landing, an increment of fuel consumption between 2.84 and 3.53 times is evaluated with respect to the standard landing. The emissions of HC and NO_x would be incremented by 2.39 times and 4.06 times, respectively, in the best case (for their specific example, based on 13R runway at King County International Airport in Seattle, USA).

(Chati and Balakrishnan, 2014) compared fuel consumption and emissions data obtained from flight data recorders (FDR) with the ICAO databank (International Civil Aviation Organization (ICAO), 2022a) in landing and takeoff procedures. They found that the ICAO data usually overestimates these values. In our work, we base our study on the ICAO data (Section 4) but, even if emissions are overestimated, we think that they are trustworthy to establish a comparison between the two missed approach methods under study.

A specific model to estimate fuel consumption and gas emissions in the case of missed approaches was presented in Murrieta-Mendoza and Botez (2016). This work is based on the Emissions Guide Book from the European Environment Agency (European Environment Agency (EEA), 2022) and its associated databases, in contrast to the BADA3 data we have used. In the example used in this paper, the missed approach burns 5.7 times the fuel needed for a successful landing, pointing out the need of operational improvements to reduce the economical and ecological impact of these supervened maneuvers.

In Rodríguez-Díaz et al. (2019), a model that considers noise and fuel consumption was proposed. The interest of a bi-objective model is that operational improvements to reduce noise impact in the airport context may increment fuel consumption. They aim to optimize both aspects by tuning airport scheduling and considering the distribution of population densities in the airport surroundings. A similar optimization model was proposed in Salah (2014) to find the best flight paths.

More detailed models, relating time, height and meteorological data, such as those proposed in Zhou et al. (2019), show that the emissions models based on ICAO data should improve their accuracy. This can be of interest to obtain accurate estimations of the ecological impact of airports, but it is not necessary to compare two missed approach methods.

To the best of our knowledge, our paper is the only one which estimates both emissions and noise effect on ground, for a classical missed approach procedure. In addition, we compare the pollution effects of this procedure with those that would be produced with the improved ARS method, allowing us to predict its ecological benefits.

3. Reinjection method for missed approach procedures

In this paper, we analyze, through simulation techniques, the positive ecological impact of adopting the ARS method for missed approach landings, as presented in Casado et al. (2021). To perform this analysis, an aircraft dynamics model is needed, including instantaneous fuel consumption in the different steps of a flight. The details of this model can be found in Carmona et al. (2022).

Hence, in this section, we proceed by first providing an overview of conventional missed approaches. Then, we briefly summarize how the proposed ARS system works. Next, we detail the developed aircraft performance and fuel consumption model.

3.1. Conventional missed approach

This work is based on the standard Instrument Approach Procedures (IAP) (Federal Aviation Administration (FAA), 2022b). In IAP, pilots are assisted by navigation aids around the runway, and they follow an instrumented approach chart which divides the approach path into segments. Geographical points define these segments and are ordered as initial, intermediate, and final segments. An additional missed approach segment can also be included.

The initial segment starts at the *Initial Approach Fix* (IAF), and it marks the end of the cruise part of a flight. Then, the intermediate segment starts at the *Intermediate Fix* (IF). This segment places the aircraft at an intermediate altitude, and it is aligned to the runway. The final segment starts at the *Final Approach Point* (FAP). In this segment, the aircraft, with navigation aids from the ground (Moir

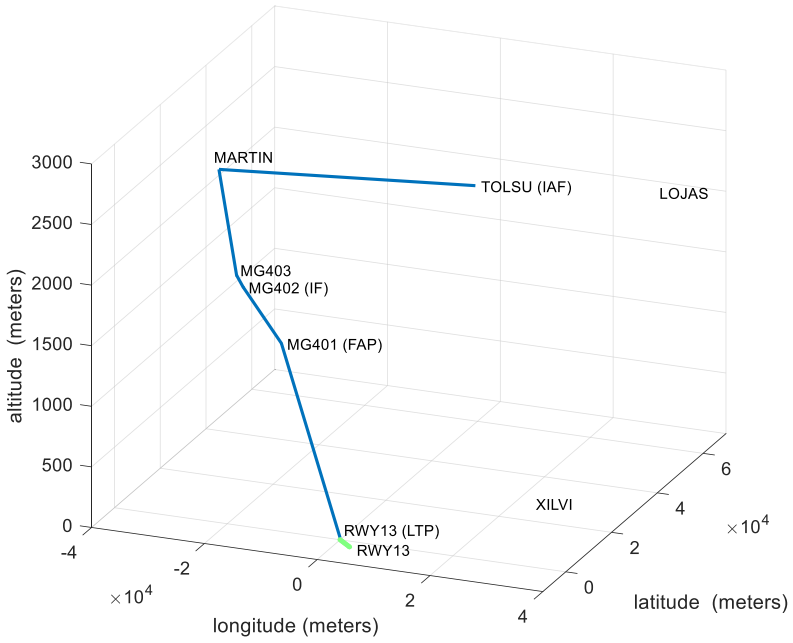

Fig. 2. Málaga airport "RWY 13" approach procedure.

Table 1
Málaga airport "RWY 13" waypoints.

Waypoint	X (m)	Y (m)	Z (m)	Speed (m/s)
LOJAS	32115.94	7950.47	2133.60	123.47
TOLSU (IAF)	3788.66	49848.85	2133.60	123.47
MARTIN	−38123.21	41103.20	2133.60	123.47
MG403	−29788.86	28279.77	1524	123.47
MG402 (IF)	−26759.25	23616.67	1524	82.31
MG401 (FAP)	−16175.05	14299.41	1280.16	82.31
RWY13 (LTP)	55.74	−53.08	15.85	72.02
RWY13	2179.44	−2035.92	15.85	25.72
XILVI	36907.56	−7831.11	670.56	113.18

et al., 2013), performs the landing maneuver. At a specific location along this path, there is a *Missed Approach Point* (MAP/MAPt) where the decision of either landing or starting a missed approach maneuver has to be taken.

To illustrate this procedure, Fig. 2 shows a 3D view of the approach to runway "RWY 13" at Málaga airport (International Civil Aviation Organization (ICAO), 2022b). Latitude and longitude are expressed in meters with respect to a reference system centered at the runway touchdown point, and altitude is expressed in meters with regard to sea level. Each division on the horizontal plane represents a 20 x 20 km^2 area. The blue line represents the path to be followed by each approaching aircraft, and the green line represents the runway. In the example, the LOJAS waypoint represents the limit of the airport airspace, and TOLSU is the IAF point. In MARTIN, aircraft are descending, and they turn to start the alignment with the runway. MG402 and MG401 are, respectively, the IF and FAP points. Table 1 summarizes the position and speed associated with each of the waypoints composing this approach procedure, where LTP (*Landing Threshold Point*) is the runway waypoint.

A missed approach (or go-around) is the procedure to be followed by an aircraft in the case a landing cannot be safely executed (Federal Aviation Administration (FAA), 2022a). Some examples may be situations of low visibility, adverse weather conditions, or the presence of unexpected obstacles on the runway. In this context, the Missed approach point (MAPt) is the point indicated in each instrument approach at which a missed approach procedure shall be executed if the required visual reference does not exist. Hence, once the pilot decides to abort the landing procedure, he/she is expected to notify to the air traffic control service (ATC) the initiation of the missed approach as soon as possible. Then, the pilot must follow the missed approach instructions indicated in the chart, or undertake an alternative maneuver as provided by the ATC. Current missed approach procedures are based on traditional radio aids-based navigation. Most of the approach charts propose a pattern that, in a best-case scenario, reroutes the aircraft to the IAF. Note that redirecting the aircraft implies additional flight time, along with a lot of workload to air controllers, who must carry out the necessary calculations to return the aircraft to the beginning of the approach.

In the case of the Málaga airport, the approach chart establishes that the aircraft must maintain approximately the same heading as that of the runway for about 20 NM, and then join the XILVI point. Once there, the aircrew must await for ATC instructions.

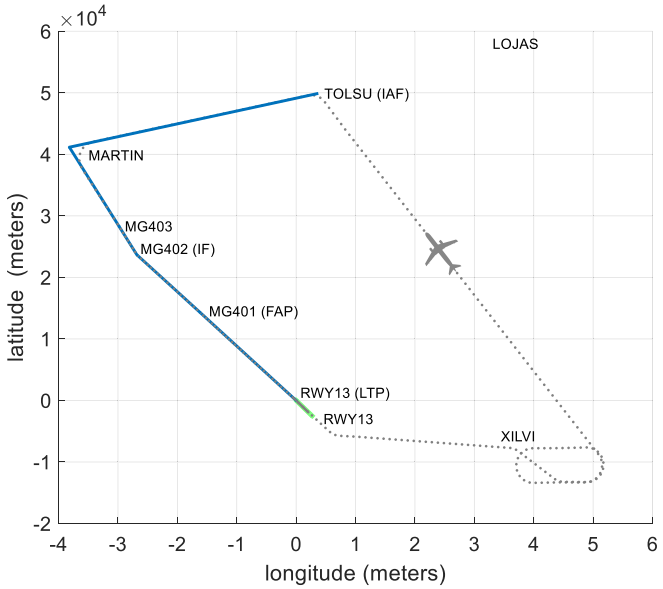

Fig. 3. Conventional missed approach maneuver at Málaga airport "RWY 13".

Fig. 3 provides an upper view of the described missed approach maneuver, assuming that air controllers have provided clearance to proceed to TOLSU (the IAF) after the aircraft has performed the holding pattern. Again, the blue line represents the approach path specified by the chart, and the dotted line indicates the path followed by the aircraft after aborting the landing (at the MAPt).

3.2. Aircraft reinjection system (ARS)

The traditional missed approach maneuver implies a high overhead. In a previous work, we proposed an optimization for this procedure, including a formal description (Casado et al., 2021), which was named Aircraft Reinjection System (ARS). A summary of the ARS procedure is presented in this subsection for a better understanding of the current work.

By default, aircraft follow the approach defined in the instrument approach chart (introduced above), but we assume that air controllers can modify, add, and remove elements in these sequences of waypoints whenever necessary. We also assume that the ATC has up-to-date information regarding the airspace situation at all times, including the position and direction of each aircraft.

ARS is initiated when the pilot of an approaching aircraft notifies the decision to abort the landing to the ATC. ARS is assisted by a computerized system that must first determine the feasibility of executing a reinjection maneuver. This is accomplished by studying the approach flow in search of a gap between two consecutive aircraft that is large enough to allow the reinjection to take place. The condition to be met is that the time difference between these two consecutive aircraft is greater than two times the minimum regulated aircraft spacing (T_s) (European Organisation for the Safety of Air Navigation (Eurocontrol), 2022b).

If the search process finds a gap satisfying the above condition, the system assumes the existence of a "ghost" aircraft in the position corresponding to the minimum allowable time behind the aircraft associated with the start of the gap. This ghost aircraft behaves exactly the same as any other aircraft executing the approach maneuver.

From this point, the ARS estimates the future position of the ghost aircraft and determines an intercepting trajectory for the aircraft to be reinjected so that both the ghost and the real aircraft will meet at a *reinjection point*. This intercepting trajectory consists of three new auxiliary waypoints that the ATC must provide to the aborting aircraft.

All the computations are performed by assuming that both the ghost and the missing approach aircraft follow Dubins trajectories (Dubins, 1957), since their computation and analysis are relatively simple. Basically, given the initial position and heading of a vehicle, Dubins curves can be used to draw a path in the 2D plane, allowing to reach a desired position and heading, under the assumption that the vehicle is moving in a straight line or using curves with a constant and predefined radius.

Dubins curves allow our ARS to estimate the time it will take for an approaching aircraft to land (Estimated Time to Arrival, ETA), the time separating two aircraft, and the position of an aircraft within a period of time. All this functionality helps to determine the existence of an available gap in the approach flow. Fig. 4 illustrates this computation, where $\mathbf{w}_1$ to $\mathbf{w}_n$ represent the waypoints for the final approach sequence, and there are four consecutive aircrafts ($\mathbf{a}_1$ to $\mathbf{a}_4$) following the landing procedure. At a given time, aircraft $\mathbf{a}_1$ decides to abort the landing. To reinsert it into the approach flow, ARS must find the location of a gap $\mathbf{g}$ before a threshold time T_1 previous to aircraft $\mathbf{a}_1$ (set as the initial search limit), and later than waypoint $\mathbf{w}_1$ (set as the final search limit). T_1 is the minimum time needed to perform the reinjection maneuver, and $\mathbf{w}_1$ is the first waypoint in the landing procedure after which reinjections can be projected. In addition, all aircraft maintain a minimum separation time T_s between them; obviously, the resulting gap also has to preserve this separation time.

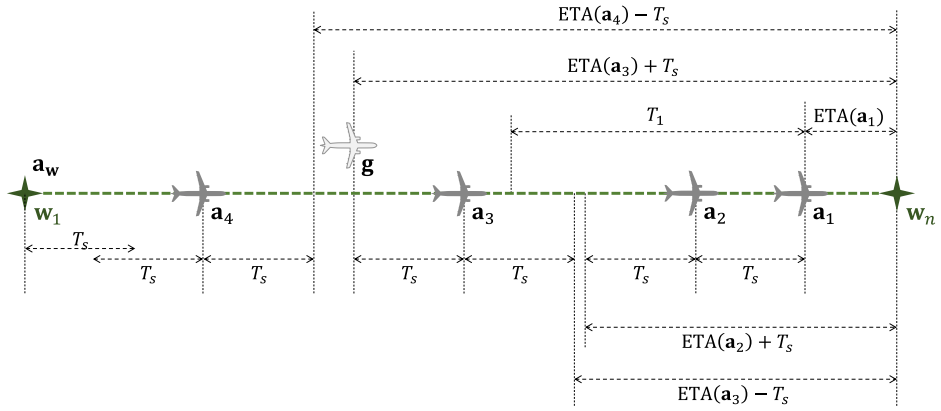

Fig. 4. Available gap computation: a missed landing by aircraft $\mathbf{a}_1$ can benefit from fast reinjection at point $\mathbf{g}$ as it meets both travel time ($> T_1$) and gap size criteria ($> 2T_s$).

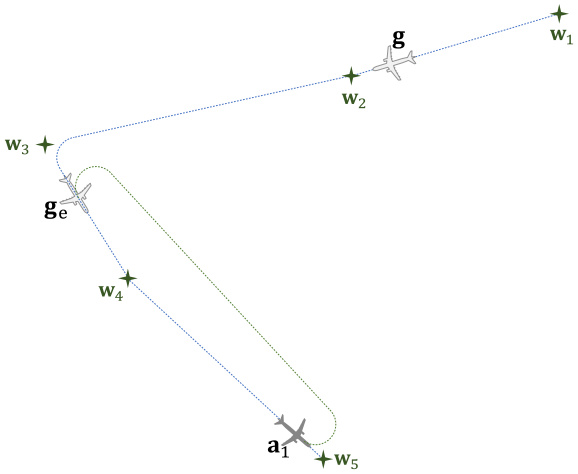

Fig. 5. Reinjection point computation (zenital view).

Next, ARS obtains the exact point at which the aircraft missing the approach would intercept a ghost aircraft located in the gap, that is, the reinjection point. Fig. 5 shows a hypothetical situation at Málaga airport, where we assume that a gap for the reinjection of aircraft $\mathbf{a}_1$ in the traffic flow (not shown here for clarity) has been found. A ghost aircraft $\mathbf{g}$ is placed on that gap, and its estimated future position ($\mathbf{g}_e$) after a certain time is obtained. This will be the point used to reinject the aircraft in the approach trajectory.

Finally, the three new waypoints that the aircraft will use to reach the reinjection point are computed. Fig. 6 shows an aircraft's trajectory (dotted line) following a missed approach maneuver according to ARS in Málaga airport. Again, for simplicity, we do not show the aircraft flow. Green dots indicate the auxiliary waypoints provided by ARS to guide the aircraft to the reinjection point.

3.3. Aircraft performance and fuel consumption model

In order to gain awareness of the implications and benefits of the ARS solution presented above, a detailed model for aircraft performance must be provided. In Carmona et al. (2022), a fuel consumption comparison between a classical missed approach procedure and ARS, in the context of the Málaga airport and the Airbus A320 aircraft model, is presented. In that paper, a performance model for fuel consumption was adapted from the Base of Aircraft DAta (BADA) (European Organisation for the Safety of Air Navigation (Eurocontrol), 2022a; Nuic et al., 2010).

BADA provides a realistic model for determining the performance of any aircraft; in particular, its family 3 aircraft performance models provide a coverage close to 100% of aircraft types, being considered a reference when attempting to achieve credible modeling of aircraft performances for the nominal part of the aircraft's operational envelope.

Thrust is directly related to fuel consumption (responsible for pollutant emissions) and aircraft noise. Let us now introduce the fuel consumption equations and algorithms presented in Carmona et al. (2022), where Eq. (1) was deduced to compute thrust (T):

$$T = D + m\left(\frac{g\dot{h}}{V} + \dot{V}\right) \tag{1}$$

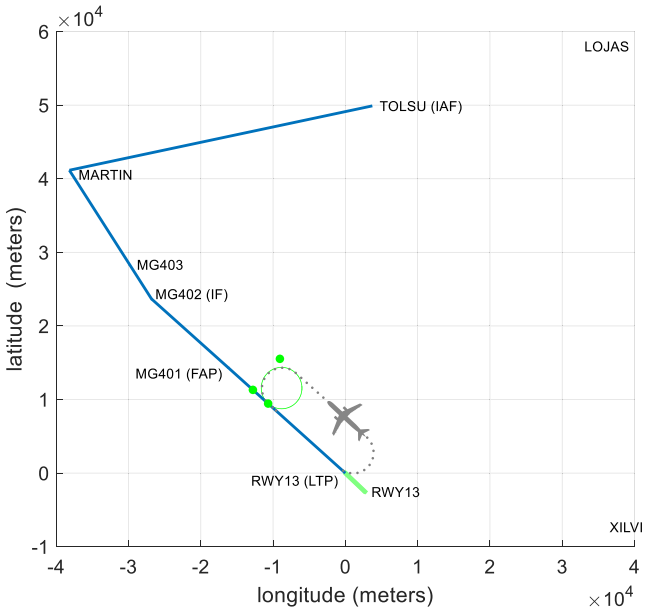

Fig. 6. Possible reinjection maneuver provided by ARS at Málaga airport "RWY 13".

BADA assumes two fuel consumption modes, called nominal and minimum, respectively. The nominal consumption model (F_{nom}) is applied in nearly all occasions. It is proportional to the propulsion force generated by the engines.

$$F_{nom} = \eta T \tag{2}$$

Such proportionality depends on the current speed (in knots), and on two constant parameters that BADA provides for each aircraft, C_{f1} and C_{f2}, as follows:

$$\eta = C_{f1}\left(1 + \frac{V}{C_{f2}}\right) \tag{3}$$

In case the aircraft is descending from a certain height (for example, above 2000 ft for the A320 aircraft), it is assumed that the pilot does not want to maintain the horizontal speed, but rather reduce it so that the engines are in idle thrust mode. In this case, the minimum fuel consumption (F_{min}) estimated by BADA depends on the geopotential height, and on two constant parameters (different from the previous ones) that BADA provides for each aircraft, C_{f3} and C_{f4}, as follows:

$$F_{min} = C_{f3}\left(1 - \frac{H_p}{C_{f4}}\right) \tag{4}$$

It is also worth mentioning that, in the troposphere (at low altitude), the geopotential height H_p can be replaced (with negligible error) by the geometric height h provided by the simulation tool used.

Applying all of the above, the instant fuel consumption F_t (kg/min) at a given time t in the approach maneuver is determined by the expression:

$$F_t = \begin{cases} F_{nom} & if\ \dot{h} \geq 0 \parallel h < 2000 \\ F_{min} & otherwise \end{cases} \tag{5}$$

Two algorithms to provide instantaneous and aggregated fuel consumption in the different flight phases are presented in Carmona et al. (2022). These algorithms are based on BADA coefficients and on the Matlab's Aerospace blockset for the air density.

4. Computation of aircraft pollutant emissions

Pollutant emissions estimations presented in this paper are based on the ICAO Aircraft Engine Emissions Databank (International Civil Aviation Organization (ICAO), 2022a), which is maintained by the European Union Aviation Safety Agency (EASA), with the analytical model equations proposed in the Boeing Fuel Flow Method 2 (BFFM2) (DuBois and Paynter, 2006).

According to the European Environment Agency (EEA) (European Environment Agency (EEA), 2022), major pollutants generated by aviation are carbon dioxide (CO_2), sulfur oxides (SO_x), nitrogen oxides (NO_x), hydrocarbons (HC), and carbon monoxide (CO).

Table 2
ICAO data for the IAE V2527-A5 engine.

Parameter (unit)	T/O	C/O	approach-landing	taxi/ground idle
NO_x EI (g/kg fuel)	23.18	19.36	9.74	5.19
HC EI (g/kg fuel)	0.03	0.03	0.07	0.14
CO EI (g/kg fuel)	0.42	0.44	2.25	11.96
Fuel Flow (kg/s)	1.049	0.873	0.328	0.134
Thrust setting (%)	100	85	30	7

Pollutants produced by aircraft mainly come from the combustion of aircraft fuel. So, the first step to compute them is to model or measure the fuel flow consumed by the aircraft during its operation. Fuel flow is usually expressed in kg/s. In this work, we will use fuel flow information provided by the consumption model presented in Section 3.3, which has been incorporated into the simulation tool that will be introduced in Section 6.1.

A typical flight consists of several phases, but we will focus on the Landing and Take-Off (LTO) cycle, which includes all the operations below 3000 ft, including taxi-out, take-off (T/O) and climb-out (C/O) at the departure phase of flight, final approach, landing, and taxi-in at the arrival phase of flight. For engine certification purposes, ICAO publishes the Aircraft Engine Emissions Databank (hereinafter, ICAO databank), which collects, for each engine model, standard fuel flows (FF) and pollutant emission indexes (EI) in the LTO cycle; these will be used in this work for the computation of some of the pollutants. EI values are expressed in g/kg of fuel, and indicate the amount (in grams) of the corresponding substance produced by the aircraft per kilogram of fuel consumed.

Concerning emissions like CO_2, SO_x, and also (non-pollutant) H_2O vapor, these are directly proportional to the fuel flow, and can be directly derived by using a set of commonly accepted EI (Kim et al., 2007). These EI are 3.149, 0.84, and 1.230 g/kg of fuel, respectively.

On the other hand, the derivation of NO_x, HC, and CO from fuel flow data is not quite direct. The reason is that the emissions of these gases depend on the engine model, and also on the working conditions due to altitude. Two similar methods have been proposed for these calculations: the BFFM2 (DuBois and Paynter, 2006; Baughcum et al., 1996), and the DLR Fuel Flow Method (Deidewig et al., 1996); the first one is considered to be in a mature development status.

The BFFM2 method starts from the data provided by the ICAO databank, being applicable to the specific engine of each aircraft. For example, the Airbus A320 is commonly equipped with two CMF56-5B4/P, or IAE V2527-A5 engines (European Environment Agency (EEA), 2022). For the last one, used in the A320-232 model, the ICAO databank provides the data shown in Table 2.

Next, BFFM2 corrects the fuel flow data provided by the ICAO databank by using a multiplication factor for each flight mode (1.01 for take-off, 1.013 for climb-out, 1.02 for approach-landing, and 1.1 for taxi/ground idle). This correction is necessary because engine certification is done on an uninstalled engine. In the case of the IAE V2527-A5 engine, the fuel flows detailed in Table 2 are corrected this way, and so the new values (in kg/s) are: 1.0595 (T/O), 0.8843 (C/O), 0.3346 (approach-landing), and 0.1474 (taxi/ground idle).

In the next step, for each pollutant (NO_x, HC, and CO), the EI values provided in the ICAO databank for each flight mode are graphically represented versus the corresponding corrected fuel flows in log–log plots, and then a curve fitting process is carried out to derive an equation that provides the EI value for any fuel flow value. Fig. 7 shows the curve resulting for the case of the NO_x when a polynomial model is used for the fitting, following Eq. (6) (FF stands for fuel flow).

$$log(EI) = 0.7468 \times log(FF) + 1.3382 \tag{6}$$

Curve fitting for HC and CO poses additional problems since ICAO reference values present two different slopes (usually a descending one first, followed by a nearly flat one). A common proposal to solve this problem consists in applying a "bi-linear" fit (DuBois and Paynter, 2006; Kim et al., 2007; Wasiuk et al., 2015), so that two different equations (one for each slope) are derived and used depending on the fuel flow region we are moving in.

Before proceeding, BFFM2 also needs to correct the fuel flow information that will be used to finally calculate the amount of pollutant emissions. The reason is that engine certification is done at standard sea level conditions. In particular, Eq. (7) corrects any fuel flow value obtained during the flight assuming that we know the actual aircraft altitude and speed:

$$W_{ff} = \frac{W_f}{\delta_{amb}} \left(\theta_{amb}^{3.8} e^{0.2Ma^2} \right) \tag{7}$$

Where W_{ff} is the corrected fuel flow (in kg/s), W_f is the modeled or measured fuel flow (in this work, it will be the F_t value defined in Section 3.3, but expressed in kg/s); δ_{amb} and θ_{amb} are, respectively, the ratios of ambient pressure and temperature over sea level pressure and temperature (by considering International Standard Atmosphere (International Standard Organization (ISO), 1975) conditions), and Ma is the Mach number (which also depends on the aircraft altitude).

Now, by using the curve fit equations previously obtained for each pollutant, the Reference Emission Index (REI) for each corrected fuel flow value (W_{ff}) is computed. In the case of NO_x, corrected fuel flow values obtained in the previous step are used as input for Eq. (6).

These REI must also be corrected to take into account the flight humidity conditions; this is achieved through Eq. (8):

$$EI = REI \sqrt{\frac{\delta_{amb}^{1.02}}{\theta_{amb}^{3.3}}} H \tag{8}$$

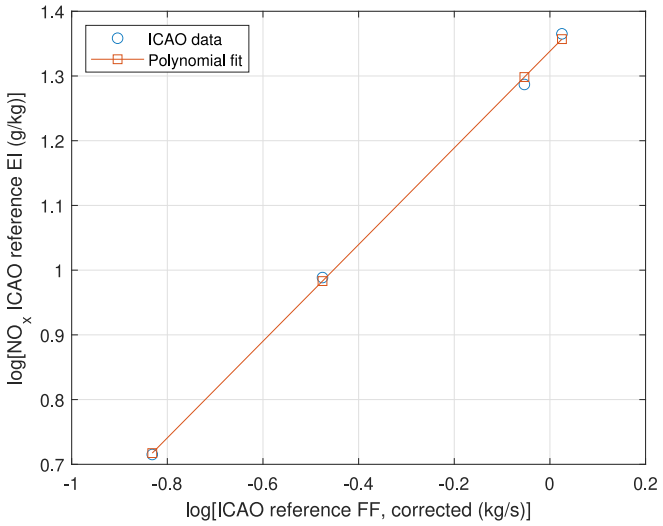

Fig. 7. NO_x EI curve fitting in BBFM2.

Where H is a humidity correction factor, defined by Eq. (9).

$$H = e^{-19(SH-0.0063)} \tag{9}$$

In this equation, SH refers to the specific humidity, or water vapor mixing ratio (mass of water vapor per mass of dry air) at flight level. On the other hand, 0.0063 is the mixing ratio under sea level standard conditions at a relative humidity of 60% (DuBois and Paynter, 2006).

As a result of Eq. (8), we get the set of final EI_i values that we will use, together with the fuel flows (W_{fi}), to finally compute (by using Eq. (10)) the amount of pollutant emissions of each type produced during the part of the flight under study:

$$E = \frac{\sum_i \left(n_e t_i W_{fi} EI_i\right)}{1000} \tag{10}$$

Where E, t_i, W_{fi}, and EI_i are expressed in kg, s, kg/s, and g/kg fuel, respectively, n_e refers to the number of engines (2 in the case of the A320), and t_i refers to the period of time for which instantaneous fuel flow values are available (in this work, $t_i = 1s$).

5. Noise model

Our analysis of the sound impact of the missed approach trajectories is based on the standard method for computing noise contours around civil airports included in the ECAC.CEAC Doc. 29 4th edition document (ECAC.CEAC, 2016a), ECAC Doc. 29 for short. In particular, we use a simplified noise model (best practice model). In these models, an aircraft is considered as a unified noise source, and they rely on aircraft performance and noise characteristics databases. In our case, the simplified developed model offers enough accuracy to compare the impact of the two considered missed approach procedures.

The noise model is based on the flight paths adopted by the aircraft that approaches to, or departs from, the target runway, and it is described as a set of segments. Thus, based on these segments, the ECAC Doc. 29 model provides a noise calculation method for a single event (that is, the noise generated in a segment) considering an observer point at a given distance d.

There are two common metrics to measure the noise level: the maximum sound pressure level reached during the event (L_{max}), measured in decibel units (dB), and the Sound Exposure Level, SEL (L_{AE}), which is a cumulative measure of the total sound energy in the event, being also measured in dB. The latter is used for aircraft noise contour modeling, and it is described in the ISO 1996-1 standard (International Standard Organization (ISO), 2016).

The ECAC Doc. 29 methodology to obtain a single event noise level is based on using the Aircraft Noise and Performance (ANP) database (Eurocontrol, 2022). This database is the primary source of aircraft noise for specific aircraft types, variants, and flight configurations (approach or departure). It provides tabulated noise metrics (such as SEL and L_{max}) depending on the distance of the observer, d, and the aircraft's power settings, P. This table is referred to as Noise-power-distance (NPD) data. Using the NPD-data and interpolation, we can obtain a baseline noise level $L_{m,b}(P,d)$ of the segment, which depends on d, P, and the type of metric L_m. From this baseline noise, it is necessary to make several corrections, which differ if the metric is L_{max} or SEL (L_{AE}):

$$L_{max,seg} = L_{max,b}(P,d) + \Delta_I(\phi) - \Lambda(\beta,l) + \Delta_{SOR} \tag{11}$$

$$L_{AE,seg} = L_{AE,b}(P,d) + \Delta_V + \Delta_I(\phi) - \Lambda(\beta,l) + \Delta_F + \Delta_{SOR} \tag{12}$$

Thus, these expressions provide segment event-level noise. Briefly, the correction terms are the following (for a complete description refer to Chapter 4 of ECAC.CEAC (2016a)):

1. Δ_V *Duration correction*: adjusts exposure levels to non-reference speeds (the ones used in the NPD-data).
2. $\Delta_I(\phi)$ *Installation effect*: takes into account the impact of the airframe configuration, particularly the location of the engines.
3. $\Lambda(\beta, l)$ *Lateral attenuation*: this term accounts for the interaction between direct and reflected sound waves, and for the effects of atmospheric non-uniformities that refract sound waves as they travel toward the observer from both sides of the aircraft.
4. Δ_F *Segment correction*: the baseline noise exposure level relates to an aircraft in continuous, straight, steady level flight; as segments are finite, this correction term accounts for their finite length.
5. Δ_{SOR} *Directivity correction*: takes into account the directionality of jet engine noise behind the ground roll segment.

When all the segment level noises of the flight path have been calculated, the maximum level L_{max} is simply the maximum of all the segments $L_{max,seg}$:

$$L_{max} = \max(L_{max,seg}) \tag{13}$$

For the SEL metric, the final sound exposure level of the flight path (L_{AE}) is calculated as the decibel sum of all the segments $L_{AE,seg}$:

$$L_{AE} = 10\log_{10}\left(\sum 10^{L_{AE,seg}/10}\right) \tag{14}$$

Based on the ECAC Doc. 29, we have implemented an Aircraft Noise Countour Modeling (ANCM) Library, which will be described in Section 6.1.

6. Performance evaluation

The aircraft re-injection procedure is a generic method applicable to any aircraft, and to any runway approach maneuver, regardless of the amount (and length) of segments composing it. It is important to note that the final benefit obtained from its application is determined by the ratio of the length of the re-injection trajectory with respect to the length of the conventional (missed approach) trajectory. On the one hand, the re-injection trajectory is primarily determined by the number of aircraft between the aircraft to be re-injected and the chosen gap, which in turn depends on the frequency with which such gaps are generated in the descent flow (policy applied by the air traffic manager). On the other hand, the conventional trajectory is prefixed in the navigation chart, and is specific to each runway. In this section, we analyze the emissions generated for a specific runway under a situation where the re-injection gap is at a representative location that is in-between worst and best case scenarios for the maneuver. Consequently, the results obtained here can be considered representative, assuming that they may vary when the re-injection situation, the runway management policy, and/or the runway itself are modified.

We conducted several simulations to study the differences between the traditional missed approach procedure and the ARS method. The simulation tool is first described, together with the simulation parameters we have used in the comparison, along with details regarding the interfacing between the simulation output and the implemented noise library (ANCM). Then, we present and analyze the obtained results.

6.1. Simulation tool and experimental setup

The flight dynamics and fuel consumption simulation model has been developed in Matlab/Simulink R2022a (The MathWorks, Inc., 2022) and it is detailed in Carmona et al. (2022).

The tool combines time-based continuous and discrete-event simulation resources available in Simulink. It includes a configurable traffic generator that provides aircraft for the simulation; these appear in the airport airspace, and proceed with the approach and landing procedures according to a programmed chart. We have considered the dynamics and the fuel consumption parameters for the Airbus A320 (see Section 3.3). The ATC, as well as the communications support that allow it to dynamically manage the sequences of waypoints followed by the aircraft, have also been modeled.

For the experiments of this work, we have considered the approach procedure for the "RWY 13" runway at Málaga airport (International Civil Aviation Organization (ICAO), 2022b) (see Section 3.1). We assume that aircraft enter the airport airspace at LOJAS (at 7,000 ft), spaced every minute and a half ($T_s = 90$ s), and that they are immediately cleared to the IAF (TOLSU) without executing any holding pattern.

As stated, to reintroduce the aircraft into the descent flow when ARS is in place, a gap must be previously generated. To this end, every certain number of aircraft, the ATC delays the next upcoming aircraft so that it joins the sequence towards the runway according to a time gap of $2T_s$ s (instead of after T_s s). Finally, we have assumed $T_1 = 240$ s, that is, with ARS an aircraft cannot be reinjected into a gap located less than 4 min behind itself in the flow (see Section 3.2).

The simulator updates the aircraft dynamics and provides as output a database with position, heading and velocity once per second throughout the simulation run. Using a Matlab script, we first obtain the horizontal and vertical velocities and accelerations; and the angle of descent, which allows us to determine the lift and drag coefficients to be applied at any given moment. Subsequently, the engine thrust and the instantaneous and aggregate fuel consumption are calculated as described in Section 3.3. Finally, we obtain the angular velocity applied in the turns, and the corresponding bank angle.

Table 3
Total fuel consumed and pollutants generated during a missed approach maneuver (in kg).

	Conventional	ARS	Saving (%)
Fuel	1.2748×10^3	257.0751	79.83
CO_2	4.0145×10^3	809.5296	79.83
SO_x	1.0709	0.2159	79.83
NO_x	40.4418	8.4414	79.13
HC (CFT)	0.1157	0.0230	80.08
HC (bi-linear fit)	0.1150	0.0228	80.18
CO (CFT)	3.4089	0.6457	81.06
CO (bi-linear fit)	3.1154	0.6173	80.18

For the computation of the resulting noise, this collection of individual positions must be transformed into rectilinear segments, as described in Chapter 3 of ECAC.CEAC (2016a). The mentioned script analyzes the sequence and generates a new segment when the aircraft's vertical/horizontal velocities or heading changes abruptly. The result is a `FlightPath` data structure where the ARS manoeuvre, consisting of 1795 3D points, has been transformed into 33 segments, and the conventional manoeuvre composed of 3764 points has been transformed into 61 segments. For each segment, the table contains the following fields:

- `segment_start_xft`, `segment_start_yft`, `segment_start_zft`: coordinates X,Y,X in feet of the start of segment.
- `segment_end_xft`, `segment_end_yft`, `segment_end_zft`: coordinates X,Y,X in feet of the end of segment.
- `thrustlbe`: engine's power in pounds.
- `bank_angle`: aircraft's bank angle.
- `op_mode`: it is 'A' arrival, or 'D' descending.
- `isRolling`: 1 if the plane is in takeoff roll or landing roll.
- `groundspeedft`: ground speed of the segment in ft/s.

In order to evaluate the noise of a flight path, we have implemented in Matlab the Aircraft Noise Contour Modeling (ANCM) library following the methodology and equations described in Chapter 4 of ECAC.CEAC (2016a)). Based on it, we developed a quite simple to use set of functions. These functions have been tested and validated with the "Reference Cases and Verification Framework" of the ECAC Doc. 29 (ECAC.CEAC, 2016b).

The main function of our library is `ANCM_GetLpath`. This function has as inputs the desired type of metric (SEL or L_{max}), the `FlightPath` data structure described above, the observer's location, the aircraft's NPD-data, and some additional information about the aircraft and atmospheric conditions.

The function returns a vector with the noise level of all the segments of the flight path (that is, Eqs. (11) and (12)). Using this vector, we can obtain a single value using Eq. (13) or (14), depending on the metric used.

Finally, the calculation of the noise contour map is straightforward using the `ANCM_GetLpath` function. We considered the area surrounding the runway that covers the flight paths (coordinate 0,0 is at the beginning of the runway). Particularly, in our experiments, the X coordinates range from −50 km to 60 km, and the Y coordinates from −20 km to 70 km. Then, iterating over these ranges using a step of 200 m, we generate a 551×451-matrix with the noise levels considering the coordinates X and Y as the observer's distance to the plane. Using this matrix, we can obtain the contour using the built-in Matlab function `countour`.

6.2. Pollutant emissions

Pollutant emissions produced by an aircraft during the execution of a missing approach have been computed from the instantaneous fuel consumption data provided by our simulation tool, and using the methodology detailed in Section 4.

As stated, for the computation of NO_x, HC, and CO with the BFFM2 technique, a curve fitting step from ICAO emission indexes (EI) and fuel flows (FF) is necessary. To fit the HC and CO EI curves, we have used the aforementioned bi-linear fit, but also the Matlab Curve Fitting Toolbox (CFT). Eqs. (15) and (16) show the resulting expressions for HC and CO, respectively, when the CFT is employed (note the high R^2 values).

$$log(EI) = 2.123e^{-0.3336 \times log(FF)} - 3.653, R^2 = 0.9946 \tag{15}$$

$$log(EI) = 1.632e^{-0.7691 \times log(FF)} - 2.013, R^2 = 0.9977 \tag{16}$$

For both low and high FF values, the EI values provided by these equations are very similar to the ones provided by the bi-linear fit, and, consequently, the derived amounts of pollutants will be very close.

Table 3 summarizes fuel consumption and pollutants emitted by the aircraft when applying the conventional missed approach procedure and ARS at Málaga airport. For HC and CO, results are shown when considering both the above fitting equations, and the bi-linear fit. Obviously, the saving percentages of the first three rows match since, as stated, the calculation of CO_2 and SO_x emissions are direct. The same is not true for the rest of the pollutants.

It can be clearly seen that, regardless of the HC and CO EI fitting procedure, ARS reduces fuel requirements and emissions of all the pollutants considered to about one-fifth of the initial values.

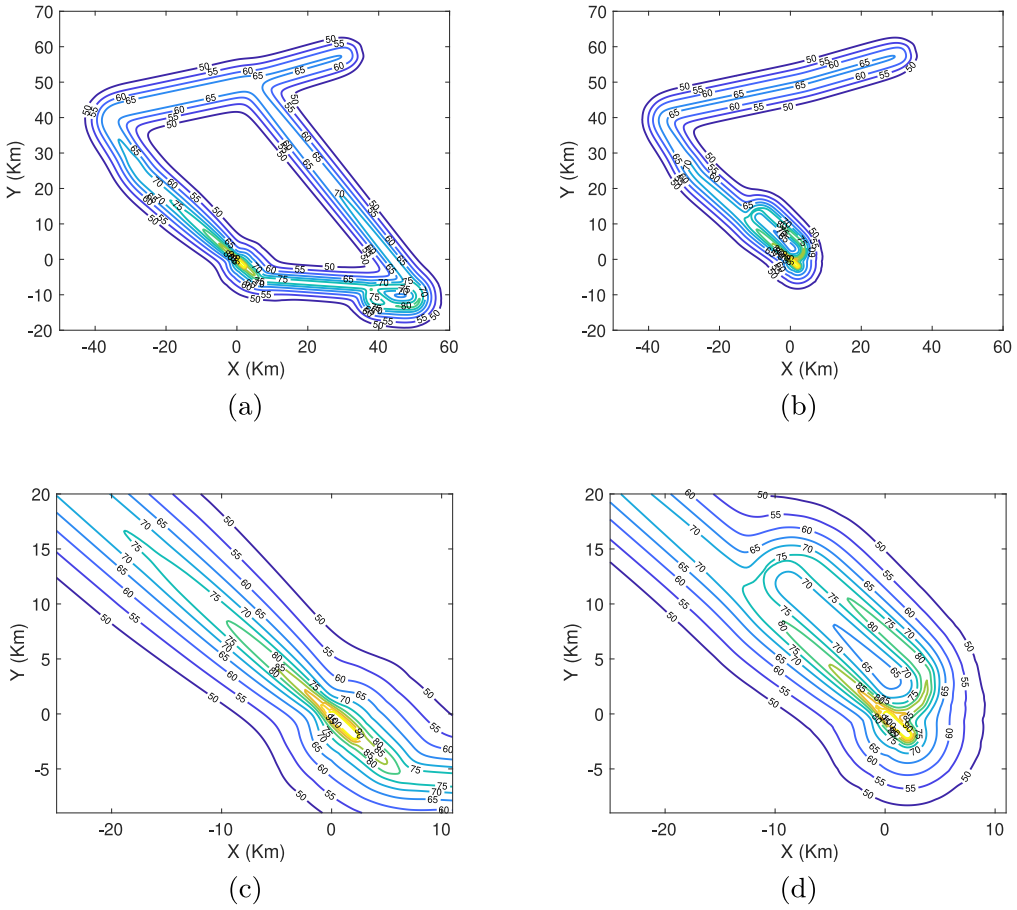

Fig. 8. SEL metric noise comparison between the conventional missed approach procedure (on the left) and ARS procedure (on the right), considering the *full* trajectory on both procedures. The second row shows a zoom of the surrounding area of the airport.

6.3. Noise analysis

In this subsection, we compare the impact of the noise generated when the aircraft follows the conventional missed approach procedure, and when it follows the ARS method. In all cases, for the NPD-data, we consider an Airbus A320-232 (V2527-A5 engines) with a reference speed V_{ref} = 270.05 ft/s. The atmospheric conditions are the standard defined on the ECAC Doc.29 (air pressure 101.325 kPa, and temperature 15° Celsius). The noise levels and contours were obtained using our ANMC library considering the `FlightPath` data structures described above.

Fig. 8 shows the contour noise maps considering the full trajectory and using the SEL metric as described in Eq. (14). Note that this metric accounts for all significant aircraft sound energy received, and it is the standard noise level used in aircraft noise contour modeling. The isolines range from 50 to 100 dB, with steps of 5 dB. On the left of the figure, we can see the noise contour when the aircraft follows a conventional missed approach procedure, and on the right, when it follows the ARS manoeuvre. It can be seen that noise is concentrated in a much smaller area with the ARS method, significantly reducing those areas where the aircraft has to make a double-pass.

In Fig. 9 we generated the same maps as in Fig. 8, but considering the L_{max} metric, that is, the maximum noise level of all the flight trajectory as described in Eq. (13). This figure displays the maximum sound intensity experienced by the observer. Consequently, the sound is more concentrated in the flight paths. Again, it can be seen that, in the ARS procedure, the noise levels are slightly lower, and, what is more important, noise is concentrated in a much smaller area.

As both flight trajectories have a common approach path, which produces the same noise map, we have generated a noise map for the non-common part of the aircraft paths to stand out the differences between the two procedures. Specifically, we removed from both `FlightPath` data structures the first 14 segments, which were exactly the same. Thus, the number of segments evaluated are 46 for the conventional procedure, and 18 for the ARS procedure. The maps are shown in Fig. 10 for the SEL noise metric. The noise reduction using ARS can be clearly seen; it only adds more noise in the area close to the airport, while the traditional method almost duplicates the noise levels after the missed approach.

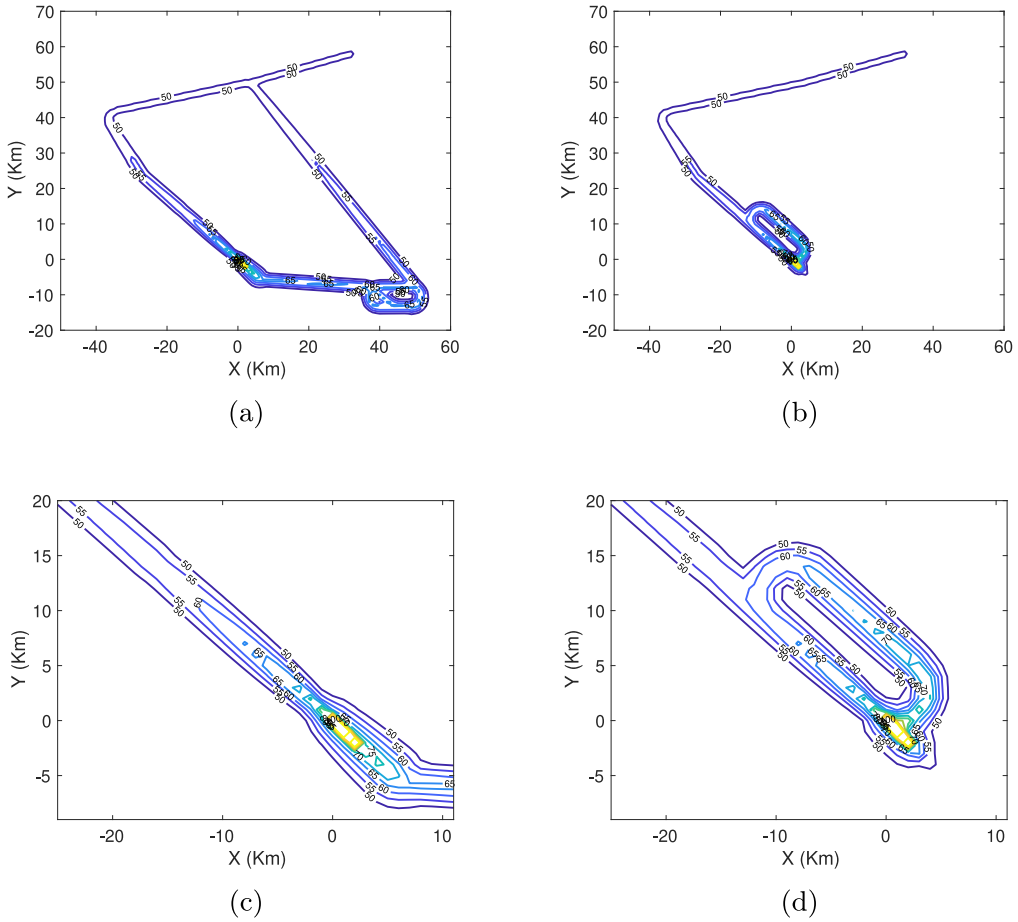

Fig. 9. L_{max} metric noise comparison between the conventional missed approach procedure (on the left) and ARS procedure (on the right) when considering the *full* trajectory on both procedures. The second row shows a zoom of the surrounding area of the airport.

From the previous noise maps, we can clearly see the difference between the noise areas of both procedures. So, to determine the difference between them, we obtained the total area (in km^2) that exceeds a given SEL threshold considering the non-common parts of both flight paths (that is, the maps of Fig. 10). The results are shown in Fig. 11 depending on the SEL threshold (from 50 dB to 100 dB). We can see that the areas for values greater than 80 dB are quite similar. These noise levels correspond to the areas close to the airport. Nevertheless, there is a very significant difference for values between 50 and 70 dB, where the ARS procedure considerably reduces the affected areas.

7. Conclusions and future works

The unstoppable growth in air operations make it necessary to improve air traffic management and to better control its impact on the environment. In this sense, in a previous work we have proposed a missed approach procedure (ARS) that allows the aircraft to land as soon as possible, thus avoiding the additional congestion on the airport airspace caused by the traditional maneuver. In addition to these improvements in flight time and airport congestion, the actual impact on citizens is also relevant. Hence, in this work we analyze in detail the benefits that ARS can offer to the quality of life of the population living in the neighborhood of the airport, and for the surrounding environment. In particular, using international databases and methods already validated and accepted in the field of aviation, we have compared the amount of noise perceived on the ground, along with the pollutant emissions produced by aircraft when executing both missed approach alternatives (traditional vs. ARS).

Simulation results using our Matlab-based models evidence a considerable reduction in the noise perceived at ground level when ARS is in place, as the affected area is reduced to about half. We have also found that there is a near 80% reduction in pollutant emissions.

As future work, it would be interesting to evaluate the loss of airport capacity when systematically planning gaps in the incoming aircraft flow versus the numerous benefits of always being able to use the ARS procedure (savings in time, fuel, noise, pollution...).

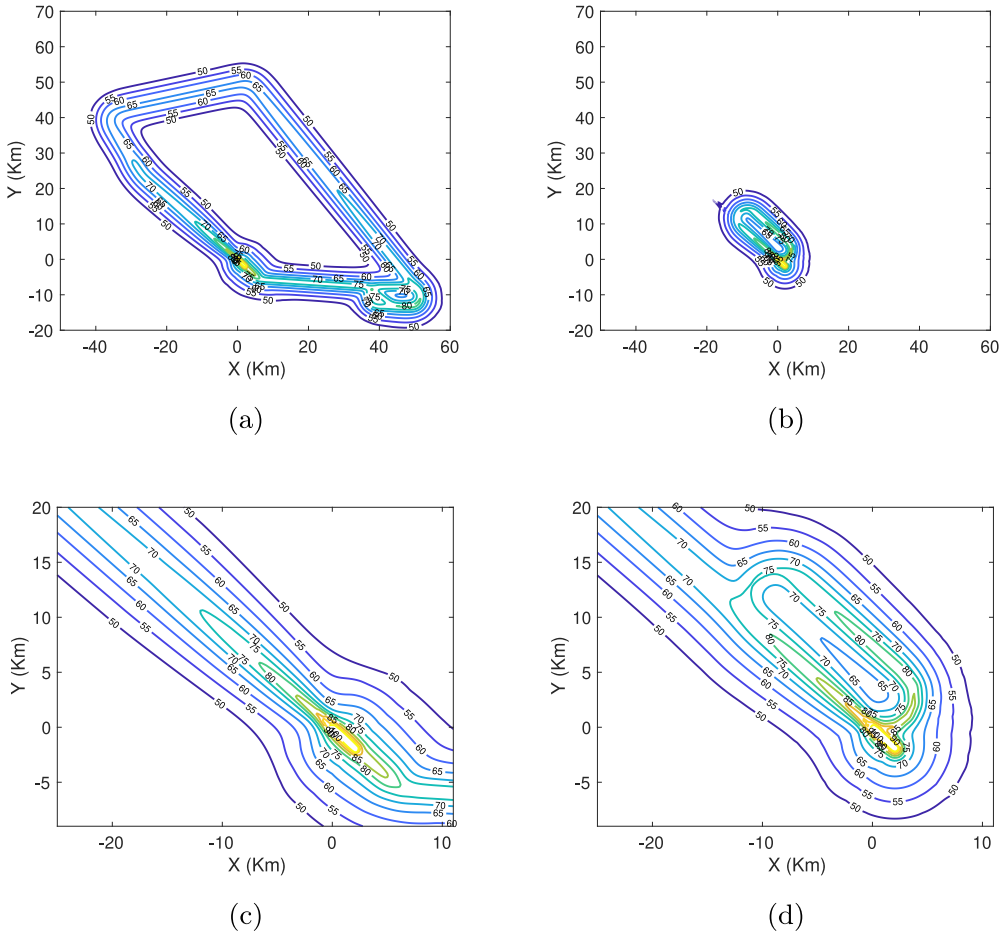

Fig. 10. SEL metric noise comparison between the conventional missed approach procedure (on the left) and ARS procedure (on the right), when considering a *partial* trajectory. The second row shows a zoom of the surrounding area of the airport.

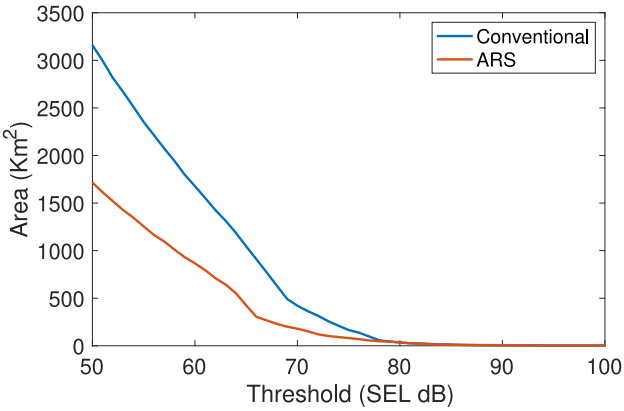

Fig. 11. Total area (km^2) exceeding a cumulative noise threshold (SEL) for the conventional missed approach procedure and the ARS procedure.

Acknowledgments

This work is derived from R&D projects PID2021-123627OB-C52 and PID2021-122580NB-I00, funded by MCIN/AEI, Spain/10.13039/501100011033 and "ERDF A way of making Europe", by the Junta de Comunidades de Castilla-La Mancha, Spain under grant SBPLY/19/180501/000159, and by the Universidad de Castilla–La Mancha, Spain under grant 2021-GRIN-31042.

References

Andarani, P., Setiyo Huboyo, H., Setyanti, D., Budiawan, W., 2018. Development of airport noise mapping using matlab software (case study: Adi Soemarmo Airport – Boyolali, Indonesia). In: Hadiyanto, Sudarno, Maryono (Eds.), E3S Web of Conferences. Vol. 31. p. 12007. http://dx.doi.org/10.1051/e3sconf/20183112007.

Basner, M., Clark, C., Hansell, A., Hileman, J.I., Janssen, S., Shepherd, K., Sparrow, V., 2017. Aviation noise impacts: state of the science. Noise Health 19 (87), 41.

Baughcum, S.L., Tritz, T.G., Henderson, S.C., Pickett, D.C., 1996. Scheduled Civil Aircraft Emission Inventories for 1992: Database Development and Analysis. Technical Report, NASA Center for Aerospace Information.

Bendtsen, K.M., Bengtsen, E., Saber, A.T., Vogel, U., 2021. A review of health effects associated with exposure to jet engine emissions in and around airports. Environ. Health 20 (1), 1–21.

Carmona, M., Casado, R., Bermúdez, A., Francisco, M.P., Boronat, P., Calafate, C.T., 2022. Fuel Savings Through Missed Approach Maneuvers Based on Aircraft Reinjection. http://dx.doi.org/10.48550/ARXIV.2207.03262, arXiv. URL: https://arxiv.org/abs/2207.03262.

Casado, R., Lopez-Lago, M., Serna, J., Bermudez, A., 2021. Enhanced missed approach procedure based on aircraft reinjection. IEEE Trans. Aerosp. Electron. Syst. 57 (6), 4149–4170. http://dx.doi.org/10.1109/TAES.2021.3082666.

Chati, Y.S., Balakrishnan, H., 2014. Analysis of aircraft fuel burn and emissions in the landing and take off cycle using operational data. In: 6th International Conference on Research in Air Transportation.

Clark, C., Paunovic, K., 2018. WHO environmental noise guidelines for the European region: a systematic review on environmental noise and quality of life, wellbeing and mental health. Int. J. Environ. Res. Public Health 15 (11), 2400.

Dancila, R., Botez, R.M., Ford, S., 2013. Fuel burn and emissions evaluation for a missed approach procedure performed by a B737-400. In: 2013 Aviation Technology, Integration, and Operations Conference. American Institute of Aeronautics and Astronautics, Reston, Virginia, http://dx.doi.org/10.2514/6.2013-4387.

Deidewig, F., Doepelheuer, A., Lecht, M., 1996. Methods to assess aircraft engine emissions in flight. In: 20th Congress of the Int. Council of the Aeronautical Sciences 1996 (ICAS), 8-13 Sept. 1996, Sorrent, Italien. pp. 131–141, URL: https://elib.dlr.de/38317/.

Dubins, L.E., 1957. On curves of minimal length with a constraint on average curvature, and with prescribed initial and terminal positions and tangents. Amer. J. Math. http://dx.doi.org/10.2307/2372560.

DuBois, D., Paynter, G., 2006. "Fuel Flow Method2" for Estimating Aircraft Emissions. SAE Technical Papers, http://dx.doi.org/10.4271/2006-01-1987.

ECAC.CEAC, 2016a. Doc 29 Volume 2: Technical Guide, fourth ed.

ECAC.CEAC, 2016b. Doc 29 Volume 3, Part 1 - Reference Cases and Verification Framework, fourth ed.

Eurocontrol, 2022. The aircraft noise and performance (ANP) database: An international data resource for aircraft noise modellers. https://www.aircraftnoisemodel.org/.

European Environment Agency (EEA), 2022. EMEP/EEA air pollutant emission inventory guidebook. https://www.eea.europa.eu/themes/air/air-pollution-sources-1/emep-eea-air-pollutant-emission-inventory-guidebook.

European Organisation for the Safety of Air Navigation (Eurocontrol), 2022a. BADA: aircraft performance model. In: EUROCONTROL – European Organisation for the Safety of Air Navigation. https://www.eurocontrol.int/model/bada.

European Organisation for the Safety of Air Navigation (Eurocontrol), 2022b. EUROCONTROL specification for time-based separation (TBS) support tool for final approach. In: EUROCONTROL – European Organisation for the Safety of Air Navigation. https://www.eurocontrol.int/publication/eurocontrol-specification-time-based-separation-tbs-support-tool-final-approach.

Federal Aviation Administration (FAA), 2022a. Aeronautical information manual (AIM). https://www.faa.gov/air_traffic/publications/atpubs/aim_html/.

Federal Aviation Administration (FAA), 2022b. Instrument procedures handbook (IPH). https://www.faa.gov/regulations_policies/handbooks_manuals/aviation/instrument_procedures_handbook/.

Filippone, A., 2016. Flight Performance Software FLIGHT. User Manual (AF-AERO-UNIMAN-2014-10). Technical Report September.

Filippone, A., 2017. Options for aircraft noise reduction on arrival and landing. Aerosp. Sci. Technol. 60, 31–38. http://dx.doi.org/10.1016/j.ast.2016.10.027.

Girvin, R., 2009. Aircraft noise-abatement and mitigation strategies. J. Air Transp. Manage. 15 (1), 14–22. http://dx.doi.org/10.1016/j.jairtraman.2008.09.012, URL: https://www.sciencedirect.com/science/article/pii/S0969699708001166.

Harada, A., Miyamoto, Y., Miyazawa, Y., Funabiki, K., 2013. Accuracy evaluation of an aircraft performance model with airliner flight data. Trans. Jpn. Soc. Aeronaut. Space Sci. Aerosp. Technol. Jpn. 11, 79–85. http://dx.doi.org/10.2322/tastj.11.79.

Homola, D., Boril, J., Smrz, V., Leuchter, J., Blasch, E., 2019. Aviation noise-pollution mitigation through redesign of aircraft departures. J. Aircr. 56 (5), 1907–1919. http://dx.doi.org/10.2514/1.C035001.

ICAO, 2016. Doc 4444 – PANS-ATM, Procedures for Air Navigation Services – Air Traffic Management, 16th ed. Montreal.

ICAO, 2017. Annex 16 to the Convention on International Civil Aviation - Environmental protection. Vol. I, eighth ed.

ICAO, 2022. Reduction of noise at source. https://www.icao.int/environmental-protection/pages/reduction-of-noise-at-source.aspx.

International Civil Aviation Organization (ICAO), 2022a. ICAO engine emissions databank. https://www.easa.europa.eu/domains/environment/icao-aircraft-engine-emissions-databank#group-easa-downloads.

International Civil Aviation Organization (ICAO), 2022b. Málaga/Costa del Sol GBAS Z RWY 13 instrument approach chart. https://aip.enaire.es/aip/contenido_AIP/AD/AD2/LEMG/LE_AD_2_LEMG_IAC_11_en.pdf.

International Standard Organization (ISO), 1975. ISO 2533:1975 standard atmosphere. https://www.iso.org/standard/7472.html.

International Standard Organization (ISO), 2016. ISO 1996-1:2016 Acoustics — Description, measurement and assessment of environmental noise — Part 1: Basic quantities and assessment procedures. https://www.iso.org/standard/59765.html.

Isermann, U., Bertsch, L., 2019. Aircraft noise immission modeling. CEAS Aeronaut. J. 10 (1), 287–311. http://dx.doi.org/10.1007/s13272-019-00374-5.

Kim, B.Y., Fleming, G.G., Lee, J.J., Waitz, I.A., Clarke, J.-P., Balasubramanian, S., Malwitz, A., Klima, K., Locke, M., Holsclaw, C.A., Maurice, L.Q., Gupta, M.L., 2007. System for assessing Aviation's Global Emissions (SAGE), Part 1: Model description and inventory results. Transp. Res. D Transp. Environ. 12 (5), 325–346. http://dx.doi.org/10.1016/j.trd.2007.03.007, URL: https://www.sciencedirect.com/science/article/pii/S1361920907000387.

Mahashabde, A., Wolfe, P., Ashok, A., Dorbian, C., He, Q., Fan, A., Lukachko, S., Mozdzanowska, A., Wollersheim, C., Barrett, S.R., Locke, M., Waitz, I.A., 2011. Assessing the environmental impacts of aircraft noise and emissions. Prog. Aerosp. Sci. 47 (1), 15–52. http://dx.doi.org/10.1016/j.paerosci.2010.04.003.

Meister, J., Schalcher, S., Wunderli, J.-M., Jäger, D., Zellmann, C., Schäffer, B., 2021. Comparison of the aircraft noise calculation programs sonair, FLULA2 and AEDT with noise measurements of single flights. Aerospace 8 (12).

Moir, I., Seabridge, A., Jukes, M., 2013. Civil Avionics Systems. John Wiley & Sons, Ltd, Chichester, http://dx.doi.org/10.1002/9781118536704.

Murrieta-Mendoza, A., Botez, R.M., 2016. New method to compute the missed approach fuel consumption and its emissions. Aeronaut. J. 120 (1228), 910–929. http://dx.doi.org/10.1017/aer.2016.37.

Nuic, A., Poles, D., Mouillet, V., 2010. BADA: An advanced aircraft performance model for present and future ATM systems. Internat. J. Adapt. Control Signal Process. 24 (10), 850–866. http://dx.doi.org/10.1002/acs.1176.

Poles, D., Nuic, A., Mouillet, V., 2010. Advanced aircraft performance modeling for ATM: Analysis of BADA model capabilities. In: 29th Digital Avionics Systems Conference. IEEE, http://dx.doi.org/10.1109/DASC.2010.5655518, 1.D.1–1–1.D.1–14.

Riley, K., Cook, R., Carr, E., Manning, B., 2021. A systematic review of the impact of commercial aircraft activity on air quality near airports. City Environ. Interact. 11, 100066. http://dx.doi.org/10.1016/j.cacint.2021.100066, URL: https://www.sciencedirect.com/science/article/pii/S2590252021000118.

Rodríguez-Díaz, A., Adenso-Díaz, B., González-Torre, P., 2019. Improving aircraft approach operations taking into account noise and fuel consumption. J. Air Transp. Manage. 77, 46–56. http://dx.doi.org/10.1016/j.jairtraman.2019.03.004.

Salah, K., 2014. Environmental impact reduction of commercial aircraft around airports. Less noise and less fuel consumption. Eur. Transp. Res. Rev. 6 (1), 71–84.

Simons, D.G., Besnea, I., Mohammadloo, T.H., Melkert, J.A., Snellen, M., 2022. Comparative assessment of measured and modelled aircraft noise around Amsterdam Airport Schiphol. Transp. Res. D Transp. Environ. 105, 103216. http://dx.doi.org/10.1016/j.trd.2022.103216, URL: https://www.sciencedirect.com/science/article/pii/S1361920922000463.

The MathWorks, Inc., 2022. Matlab. https://www.mathworks.com/products/matlab.html.

Wasiuk, D., Lowenberg, M., Shallcross, D., 2015. An aircraft performance model implementation for the estimation of global and regional commercial aviation fuel burn and emissions. Transp. Res. D Transp. Environ. 35, 142–159. http://dx.doi.org/10.1016/j.trd.2014.11.022, URL: https://www.sciencedirect.com/science/article/pii/S1361920914001850.

W.H.O., W.H.O., et al., 2011. Burden of Disease from Environmental Noise: Quantification of Healthy Life Years Lost in Europe. World Health Organization. Regional Office for Europe.

Zhou, Y., Jiao, Y., Lang, J., Chen, D., Huang, C., Wei, P., Li, S., Cheng, S., 2019. Improved estimation of air pollutant emissions from landing and takeoff cycles of civil aircraft in China. Environ. Pollut. 249, 463–471. http://dx.doi.org/10.1016/j.envpol.2019.03.088, URL: https://www.sciencedirect.com/science/article/pii/S0269749119306797.